COMPRESSION STRENGTH OF COMPOSITE PRIMARY STRUCTURAL COMPONENTS

Semiannual Status Report

Eric R. Johnson
Principal Investigator

May 1, 1988 to October 31, 1988

Virginia Polytechnic Institute and State University
Aerospace and Ocean Engineering
Blacksburg, Virginia 24061-0203

NASA Grant NAG1-537

INTRODUCTION

The focus of research activities under NASA Grant NAG1-537 is the geometrically nonlinear response and failure of thin-walled structural components made from advanced composite materials. The research is applicable to primary structural components in flight vehicle structures that are laminated from graphite-epoxy unidirectional tape. The two projects under investigation involve the buckling, postbuckling, and failure of structures subject to axial compression. One project is concerned with the analysis of delamination during crippling of open section stiffeners, and the other is concerned with the influence of dropped plies on the response and failure of laminated plates. Both experimental and theoretical methods are used to study the fundamental mechanisms limiting the load-carrying capacity of these components. The experimental activities have been accomplished in cooperation with the Structural Mechanics Branch of the NASA Langley Research Center using their facilities.

INTERLAMINAR STRESS POST-PROCESSOR

The purpose of the interlaminar stress post-processor development is to evaluate the delamination failure mode of the crippling specimens in Ref. 1. The specimens tested in Ref. 1 were thin-walled open section stiffeners subject to axial compression, and the analysis of their geometrically nonlinear response was done using the STAGS (STructural Analysis of General Shells) computer code. The STAGS code was used to evaluate in-plane stresses and intralamina modes of failure initiation, but interlaminar stress response and the prediction of delamination was outside its current capability.

The STAGS code did not have the capability to predict interlaminar stresses because it is based on virtual work and assumed displacements for thin shell elements; i.e., structural configurations for which plane stress approximations are appropriate. A conventional engineering practice is to estimate the out-of-plane stress components from the three-dimensional elasticity equations of equilibrium, using the linear distribution through the thickness of the in-plane stress components. This procedure, however, requires displacement derivatives of order 2p, where p designates the order of the highest displacement derivatives in the internal virtual work expression (or strain energy density increment). Derivatives of order 2p of the interpolation functions for the displacements within an element are meaningless. Consequently, the methodology of the interlaminar stress post-processor development is to construct higher order interpolations of the displacement field over an assembly of elements, and then take order 2p derivatives of it.

Two interpolation techniques for approximating a displacement function from discrete data have been attempted. The first technique constructed a truncated Fourier Series representation, and the second technique constructed a Chebyshev polynomial representation. The merits of these techniques were judged by sampling a known analytic function at discrete points in its domain, and computing the errors between the interpolation of the function and its first four derivatives and the known exact values.

The analytic function used for the comparison is an approximation to the buckling mode of a uniaxially compressed, orthotropic, rectangular plate whose loaded edges are clamped, one unloaded edge is clamped, and the other unloaded edge is free. The buckling mode is the out-of-plane displacement $w(x,y)$ of the plate, in which the x-axis is along the length of the plate in the direction of the applied load, and the y-axis is across the width of the plate. The length of the plate in this example is two-and-a-half times its width. To make the buckling mode of definite value, it was normalized such that the maximum out-of-plane displacement at the middle of the free edge was equal to the thickness of the plate. This particular displacement function was selected because it is similar to the displacement response of a stiffener's flange during local buckling. The exact function and details of the construction of the Fourier Series are given in Ref. 2. (Reference 2 is also in the appendix of this report.)

Fourier Series Representation

The norms of the Fourier Series approximation to the displacement and its first four derivatives using a 21 x 11 rectangular grid of sample points are given in the third column of Table 1. This grid consists of twenty-one equally spaced locations along the length of the plate, and eleven equally spaced locations across the width. The norm of a quantity is defined to be the square root of the sum of the squares of that quantity over all grid points. The norms of the exact function and its first four derivatives are shown in the second column of Table 1, and the percent error of the approximate norm to the exact is given in the fourth column. Very large errors in some of the third and fourth derivatives computed from the Fourier Series occur. Third and fourth derivatives are required to calculate the interlaminar shear and normal stresses, respectively. Although not presented here, increasing the grid to 41 x 21 sample points did not improve the computation of the third and fourth derivatives. Thus, the Fourier Series method of computing interlaminar shear and normal stresses from discrete displacement data, as provided by a finite element computer code for example, would be too inaccurate for engineering purposes.

The reason for the inaccuracies in the higher derivative data computed from the Fourier Series is due to Gibbs phenomena; i.e., a "ringing" in the truncated Fourier Series representation of the function in the vicinity of the boundaries of the plate. Since the buckling displacement and its derivative normal to the edge are zero on the three clamped edges, and are non-zero on the free edge, the periodic extension of this function, or the protracted function, exhibits discontinuities. Consequently, the infinite series convergence is non-uniform at the plate boundaries, and the truncated series exhibits oscillations, or ringing, in the vicinity of the boundaries.

Efforts were made to reduce the Gibbs phenomena. A smooth protracted function was constructed from the discrete displacement data by defining a function from the grid point data along the free edge that interpolated the displacement and its normal derivative there, and also satisfied the vanishing of the displacement and normal derivative along the remaining three boundaries (see Ref. 2). This function defined by the free edge data was subtracted from the original displacement field to define the smooth protracted function, and then a Fourier Series was constructed by sampling the smooth protracted function at the grid points. This approach

substantially reduced the Gibbs phenomena in the displacement and its first two derivatives, but the third and fourth derivative data were still very oscillatory near the free edge. In addition, smoothing of the higher derivative data was used to reduce the oscillation in the data, but this did not substantially reduce the errors. The errors reported in Table 1 are based on defining a smooth protracted function and smoothing the higher derivative data.

Chebyshev Series Representation

The norms of displacement and its first four derivatives for a 20 x 10 rectangular grid of Chebyshev points are given in the third column of Table 2. The twenty locations along the length of the plate correspond to the zeros of the twentieth Chebyshev polynomial, and the ten locations across the width correspond to the zeros of the tenth Chebyshev polynomial. The spacing of grid points is not equal along the length or width. Thus, the grid of sample points in the Chebyshev representation are not the same spatial locations as in the Fourier Series representation; so the exact norms shown in the second column of Table 2 do not equal those in the second column of Table 1. The absolute value of the percentage errors between the approximate and exact norms with respect to the exact are given in column four of Table 2. The percentage errors are remarkably small with respect to those computed by the Fourier Series representation, with the maximum error being 0.1% in the norm of the fourth derivative with respect to y. For this example then, the Chebyshev representation gives superior results.

POSTBUCKLING OF DROPPED-PLY LAMINATES

Laminated panels containing dropped plies (terminated internal plies) are common in aircraft wing construction in which the skin stiffness is reduced from root to tip. Dropped plies result in a thickness discontinuity which can reduce the strength of the panel. Experiments reported in Ref. 3 showed that a 12% - 50% reduction in compression strength can occur for buckling susceptible specimens with respect to buckling resistant specimens having the same dropped-ply laminate construction. Thus, the influence of the dropped-ply thickness discontinuity on the postbuckling response and failure is an important issue, and the focus of this project under the current grant.

Kantrovich's method is being used to compute the geometrically nonlinear response of laminates containing dropped plies. For a plate with simply supported unloaded edges, the displacements are expanded in a Fourier Series in the width-wise coordinate y, which is the coordinate normal to the unloaded edges. The trigonometric basis functions of the Fourier Series satisfy the kinematic conditions along the simply supported edge. Ordinary differential equations in the axial coordinate x are derived in Kantrovich's method for the "coefficients", or generalized coordinates, of the trigonometric basis functions in the Fourier expansion via the principle of virtual work. In addition to boundary conditions at the two loaded edges of the plate, transition conditions at the dropped-ply location result. (The dropped-ply site is modelled as a step change in the thickness of the plate.) Thus, the mathematical problem reduces from a solution of nonlinear partial differential equations to the solution of a set nonlinear ordinary differential equations with multipoint boundary conditions. The number of

ordinary differential equations depends on the number of terms, denoted by N, retained in the Fourier expansion.

The stability equations to compute the buckling load for the laminated plate with a symmetric thickness change, and subject to uniaxial in-plane compression, are a linear set of ordinary differential equations with multipoint boundary conditions as obtained by Kantrovich's method. This eigenvalue problem was solved for thick, specially orthotropic, dropped-ply plates by finding complementary functions satisfying the homogeneous differential equations, and then imposing the boundary conditions to get the characteristic equation for the eigenvalues. A sixth-order transverse shear deformation plate theory was used. The results are documented in Ref. 4, and show that transverse shearing deformations can significantly affect the buckling load and the mode for thick laminated plates having a step change in thickness relative to a Kirchhoff plate theory. (Reference 4 is also in the appendix of this report.)

The major drawback to the solution methodology employed in Ref. 4 was the computation of the complementary functions, which would be difficult to do for a large number (N) of terms retained in the Fourier expansion. Also, the transcendental terms in the characteristic equation for larger values of N would lead to numerically ill-conditioned computations for the eigenvalues.

Currently work is in progress to solve the postbuckling problem for the dropped-ply laminate using the knowledge gained in the solution to the buckling problem. Newton's method will have to be used to iterate for the solution at each load step in the postbuckling analysis. The linear ordinary differential operators that need to be solved in each iteration are very similar to the differential operators of the buckling problem. Instead of seeking complementary functions, and then general solutions, to these linear equations, we are using the field method (Ref. 5) to numerically obtain the linear solutions. The field method is a way to solve multipoint boundary value problems for linear, ordinary differential equations using initial value integration schemes (like Runge-Kutta). "Field relations" are used to stabilize the numerical integration against exponentially growing homogeneous solutions. Since this method is applied to the governing differential equations, derivatives the order of the differential equations are computed directly. This permits the computation of interlaminar stresses from the three-dimensional elasticity equations of equilibrium once the plate solution is obtained by the field method. Thus, in addition to computing the postbuckling response, the delamination failure modes of the dropped ply specimens in Ref. 3 can also be studied.

REFERENCES

1. Bonanni, David L., Johnson, Eric R. and Starnes, James H., Jr., "Local Buckling and Crippling of Thin-Walled Graphite-Epoxy Stiffeners," in the proceedings of the AIAA/ASME/ASCE/AHS 29th Structures, Structural Dynamics and Materials Conference, Part 1, April 18-20, 1988, Williamsburg, VA, pp. 313-323; AIAA Paper No. 88-2251.

2. Johnson, Eric R. and Bonanni, David L., "Order 2p Derivatives from p-Differentiable Finite Element Solutions by a Spectral Method," in CARS &

FOF' 88 Conference Proceedings, Vol. 1, edited by J.G. Eisley, Springer-Verlag New York Inc., in press.

3. Curry, J.M., Johnson, E.R. and Starnes, J.H., Jr., "Effect of Ply Drop-Offs on the Strength of Graphite-Epoxy Laminates," Center for Composite Materials and Structures Report CCMS 86-07 and College of Engineering Report VPI-E-86-27, Virginia Polytechnic Institute and State University, Blacksburg, VA 24061, December 1986.

4. Johnson, Eric R. and Davila, Carlos G., "Compression Buckling of Thick Orthotropic Plates with a Step Thickness Change," accepted for publication in the proceedings of the Twelfth Canadian Congress of Applied Mechanics, May 28-June 2, 1989, Carleton University, Ottawa, Canada.

5. Jordan, P.F. and Shelley, P.E., "Stabilization of Unstable Two-Point Boundary Value Problems," AIAA Journal, Vol. 4, May 1966, pp. 923-924.

Table 1 Norms of the displacement and its first four derivatives by the Fourier representation on a 21 x 11 grid.

Derivative	Norms Exact	Norms Approx.	Percent Error
w	0.3225	0.3126	3.1
w,x	0.4680	0.4469	4.5
w,y	0.6940	0.6819	1.8
w,xx	1.176	1.028	12.6
w,xy	1.007	0.9749	3.2
w,yy	1.457	1.438	1.3
w,xxx	2.956	18.19	-515.3
w,xxy	2.531	2.232	11.8
w,xyy	2.114	2.055	2.8
w,yyy	4.848	4.398	9.3
w,xxxx	7.429	991.1	-13241.0
w,xxxy	6.361	43.88	-589.8
w,xxyy	5.314	4.765	10.3
w,xyyy	7.035	6.287	10.6
w,yyyy	14.66	41.64	-184.0

Table 2 Norms of the displacement and its first four derivatives by the Chebyshev representation on a 20 x 10 grid.

Derivative	Norms Exact	Norms Approx.	Percent Error
w	0.3230	0.3230	≈0
w,x	0.5065	0.5065	≈0
w,y	0.5785	0.5785	≈0
w,xx	1.592	1.592	≈0
w,xy	0.9070	0.9070	≈0
w,yy	1.329	1.329	0.0066
w,xxx	3.199	3.199	≈0
w,xxy	2.852	2.852	≈0
w,xyy	2.084	2.084	0.0066
w,yyy	4.445	4.444	0.0104
w,xxxx	10.06	10.06	≈0
w,xxxy	5.729	5.729	≈0
w,xxyy	6.551	6.551	0.0066
w,xyyy	6.969	6.969	0.0104
w,yyyy	14.18	14.17	0.1016

APPENDIX

Order 2p Derivatives from p-Differentiable Finite Element Solutions by a Spectral Method

by

Eric R. Johnson and David L. Bonanni
Virginia Polytechnic Institute and State University
Blacksburg, VA 24061-0203

July 7, 1983

Presented at CAD/CAM, Robotics and
Factories of the Future
Third International Conference
Southfield, Michigan
August 14-17, 1988

Order 2p Derivatives from p-Differentiable Finite Element Solutions by a Spectral Method

Eric R. Johnson and David L. Bonanni

Aerospace and Ocean Engineering Department
Virginia Polytechnic Institute and State University
Blacksburg, Virginia 24061-0203

Summary

The displacements and their first p-1 derivatives are continuous across element boundaries for conforming elements in the finite element representation of a C^{p-1} variational problem. That is, a variational problem in which the highest derivative of the state variable in the functional is order p. For plate bending problems based on Kirchhoff theory, the state variable is the out-of-plane displacement and p = 2. This paper discusses the problem of computing derivatives of order 2p for a laminated composite plate from the assembly of elements in which the element displacements have p-differentiablity within the element. Order 2p derivatives of the out-of-plane displacement are necessary to compute interlaminar stresses.

Introduction

Delamination is a common failure mode in laminated composite structures. However, most finite element analyses for built-up structural components are based on Kirchhoff theory which assumes a state of plane stress and hence neglects interlaminar stresses. The engineering approach to compute the interlaminar stresses from the Kirchhoff theory is to integrate the three-dimensional equilibrium equations for the out-of-plane stress components using the linear distribution in the thickness coordinate of the in-plane stress components from the Kirchhoff theory [1]. This is difficult to implement in finite element solutions because such a proceedure implies that fourth order derivatives of the out-of-plane displacement are required when the finite element formulation only requires continuity of the displacement and its first derivatives between elements. Thus taking fourth order derivatives of the finite element representation of the displacements within an element is meaningless. The method presented in this paper uses the Discrete Fourier Transform of the finite element displacement data over the whole domain of the plate to determine a finite number of Fourier Series coefficients for the displacement. The truncated Fourier Series is differentiated to obtain the higher order derivatives. This approach to

compute derivatives from discrete data was used by Tielking and Schapery [2] in a shell contact problem.

Spectral Method

The spectral method is used in this paper as an efficient computational tool to determine Fourier Series coefficients from discrete displacement data. The method is reviewed in the context of representing the out-of-plane displacement of a plate. Designate this displacement as $f(x,y)$, $0 \leq x \leq a$, and $0 \leq y \leq b$, where a and b denote the length and width , respectively, of a rectangular plate. It is assumed the plate is modelled in the finite element analysis such that there are M equally spaced intervals between nodes in the x-direction, and N equally spaced intervals between nodes in the y-direction, where M and N are even integers. The extension of the function $f(x,y)$ outside the domain of the plate, or the protracted function, is defined by periodicity in x with period a, and periodicity in y with period b. The protracted function and its first derivatives are assumed to be continuous; i.e., $f(x,y)$ has C^1 continuity.

The complex Fourier Series representation of $f(x,y)$ is

$$f(x,y) = \sum_{m=-\infty}^{\infty} \sum_{n=-\infty}^{\infty} c(m,n) \exp[2\pi i(mx/a + ny/b)], \quad i = \sqrt{-1}. \tag{1}$$

Evaluating $f(x,y)$ in eqn. (1) at the nodes $(x_j, y_k) = (ja/M, kb/N)$, where $j = 0,1,2,\ldots,M-1$, and $k = 0,1,2,\ldots,N-1$, we obtain

$$f(j,k) = \sum_{m=-\infty}^{\infty} \sum_{n=-\infty}^{\infty} c(m,n)\, W_M^{jm}\, W_N^{kn} \tag{2}$$

in which $f(j,k) = f(x_j, y_k)$, and $W_M = \exp(2\pi i/M)$ and $W_N = \exp(2\pi i/N)$ are the weighting kernels. The doubly infinite sum in eqn. (2) may be restructured in the form

$$f(j,k) = \sum_{m=0}^{M-1} \sum_{n=0}^{N-1} c_p(m,n)\, W_M^{jm}\, W_N^{kn} \tag{3}$$

where

$$c_p(m,n) = \sum_{r=-\infty}^{\infty} \sum_{s=-\infty}^{\infty} c(m + Mr,\, n + Ns); \quad \begin{matrix} m = 0,1,\ldots,M-1 \\ n = 0,1,\ldots,N-1 \end{matrix} \tag{4}$$

Eqn. (3) defines the Inverse Discrete Fourier Transform, and shows that the sequences $f(j,k)$ and $c_p(m,n)$ are Discrete Fourier Transform (DFT) pairs.

Thus, the sequence $c_p(m,n)$ is determined from the DFT of the sequence $f(j,k)$ by the formula

$$c_p(m,n) = 1/(MN) \cdot \sum_{j=0}^{M-1} \sum_{k=0}^{N-1} f(j,k)\, W_M^{-mj}\, W_N^{-nk}; \quad \begin{matrix} m = 0,1,\ldots,M-1 \\ n = 0,1,\ldots,N-1 \end{matrix} \qquad (5)$$

The Fast Fourier Transform algorithm can be used to compute the DFT of the sequence $f(j,k)$ in eqn. (5).

For large values of M and N in eqn. (4), the terms $c_p(m,n)$ are good approximations to the Fourier Series coefficients. The dominate Fourier coefficients in the infinite sums on the right-hand-side of eqn. (4) occur for values of r and s equal to either -1 or 0. Thus

$$c(m,n) \approx c_p[m+M \cdot H(-m),\ n+N \cdot H(-n)], \quad |m| < M/2 \text{ and } |n| < N/2 \qquad (6)$$

in which $H(\ ) = 1$ if the argument is > 0, and $H(\ ) = 0$ if the argument is ≤ 0. If $m = \pm M/2$ or $n = \pm N/2$, then eqn. (6) is valid if c_p is divided by two. If both $m = \pm M/2$ and $n = \pm N/2$, then eqn. (6) is valid if c_p is divided by four. With the Fourier coefficients approximated by eqn. (6), the truncated Fourier Series representation of $f(x,y)$ is

$$f(x,y) \approx \sum_{m=-M/2}^{M/2} \sum_{n=-N/2}^{N/2} c(m,n)\, \exp[2\pi i(mx/a + ny/b)] \qquad (7)$$

Orthotropic Plate Example

Although the objective is to use the spectral method to compute derivatives of finite element data, the methodology is tested here by sampling an analytic function, computing its derivatives by the spectral method, and comparing derivatives computed by the spectral method to exact values. The analytic function chosen for this purpose is an approximate buckling mode for a rectangular plate subject to uniform compression at $x = 0$ and $x = a$. The plate is clamped along edges $x = 0$, $x = a$, and $y = 0$, and is free along the edge $y = b$. It is laminated from AS4/3502 graphite-epoxy tape with material properties $E_1 = 18.5$ msi, $E_2 = 1.64$ msi, $\nu_{12} = 0.30$, and $G_{12} = 0.87$ msi. The laminate consists of sixteen plies with a stacking sequence $[\pm 45/0/90]_{2s}$. The plate's dimensions are $a = 2.5$ in., $b = 1.0$ in., and the thickness is 0.080 in. The approximate analysis neglects the twist curvature-bending moment coupling of anisotropic plate theory, and uses Kantrovich's method in Trefftz's criterion to determine the buckling mode.

The buckling mode is normalized such that the maximum displacement at x = a/2 and y = b is equal to the thickness of the plate. The result is

$$w(x,y) = [1 - \cos(2\pi x/a)]\,[K_1\exp(\alpha y/b) + K_2\exp(\alpha y/b) + K_3\sin(\beta y/b) + K_4\cos(\beta y/b)] \quad (8)$$

where $K_1 = 5.6196 \times 10^{-4}$ in., $K_2 = 1.4571 \times 10^{-2}$ in., $K_3 = 2.4399 \times 10^{-2}$ in., $K_4 = -1.5133 \times 10^{-2}$ in., $\alpha = 3.0919$, and $\beta = 1.7753$.

The protracted function obtained from w(x,y) in eqn. (8), and its first partial derivative in y (denoted $w_{,y}$), are discontinuous at integer multiples of y = b. The truncated Fourier Series representation of w(x,y) would exhibit Gibbs phenomena near y = b, because of the nonuniform convergence at the discontinuity. To avoid the Gibbs phenomena, a polynomial function $w_p(x,y)$ is defined such that the difference function

$$f(x,y) = w(x,y) - w_p(x,y) \quad (9)$$

has the C^1 continuity properties discussed previously. The polynomial is selected to match the essential boundary conditions, i.e., w and its derivative normal to the edge, at the nodal points along the edge. For this example, the polynomial selected is

$$w_p(x,y) = x^2(x-a)^2y^2[f(x) + (y-b)g(x)] \quad (10)$$

in which f(x) and g(x) are Mth order interpolation polynomials. Polynomials f(x) and g(x) are defined by the M+1 nodal values of $w(x_j,b)$ and $w_{,y}(x_j,b)$, respectively, where $x_j = ja/M$, j = 0,1,...,M.

Denoting the approximation to the function w(x,y) as $\tilde{w}(x,y)$, then $\tilde{w}(x,y)$ is the sum of $w_p(x,y)$ and the approximation of f(x,y) as given by eqn. (7). The norms of $w(x_j,y_k)$ and $\tilde{w}(x_j,y_k)$, and their first four derivatives, are compared in Table 1 for M = 20 and N = 10. The norm of a discrete function is defined as the square root of the sum of the squares of the discrete function values over all nodal points. The approximate function norms in Table 1 are determined from smoothed data values; i.e., for an interior node, the value of the function at that point is replaced by the average value of the function at the node plus the function values at the eight adjacent nodes. The smoothed data gives slightly better results than raw data. It is clear from Table 1 that for derivatives of the same order

errors increase as the number of differentiations in x increase with respect to those in y. Also, errors increase with increasing order of the derivative. It is likely that the high order interpolation polynomials f(x) and g(x) cause severe oscillations in the higher order derivative data, especially for derivatives in x. A least squares fit of lower order polynomials for f(x) and g(x) may decrease this oscillation in higher order derivatives with respect to x. However, continuity of the protracted function at the node points along y = b is sacrificed if lower order polynomials for f(x) and g(x) are used. The loss of continuity leads to Gibbs phenomena, which can also result in severe oscillations.

Acknowledgement

The research for this paper sponsored by NASA Grant NAG1-537.

References

1. Bonanni, D. L., Johnson, E. R., and Starnes, J. H., Jr., "Local Buckling and Crippling of Composite Stiffener Sections," Center for Composite Materials and Structures Report CCMS-88-08, Virginia Polytechnic Institute and State University, Blacksburg, VA 24061, pp. 126-136.

2. Tielking, J. T., and Shapery, R. A., "A Method for Shell Contact Analysis," Computer Methods in Applied Mechanics and Engineering, Vol. 26, 1981, pp. 181-195.

Table 1 Norms of the exact and approximate displacements and there first four derivatives on a 21 by 11 rectangular grid

	Norms		Percent
Derivative	Exact	Approximate	Error
w	0.322498	0.312629	3.06
w,x	0.467957	0.446934	4.49
w,y	0.694032	0.681892	1.75
w,xx	1.17610	1.02820	12.58
w,xy	1.00707	0.974863	3.20
w,yy	1.45716	1.43758	1.34
w,xxx	2.95587	18.1876	-515.30
w,xxy	2.53104	2.23268	11.79
w,xyy	2.11439	2.05507	2.81
w,yyy	4.84802	4.39844	9.27
w,xxxx	7.42892	991.130	-13,241.
w,xxxy	6.36120	43.8807	-589.82
w,xxyy	5.31405	4.76466	10.34
w,xyyy	7.03466	6.28657	10.63
w,yyyy	14.6630	41.6433	-184.00

Compression Buckling of Thick Orthotropic Plates with a Step Thickness Change

Eric R. Johnson and Carlos G. Davila
Aerospace and Ocean Engineering
Virginia Polytechnic Institute and State University
Blacksburg, Virginia 24061-0203 USA

November 2, 1988

A paper submitted to the
Twelfth Canadian Congress of Applied Mechanics
May 28 - June 2, 1989
Carleton University
Ottawa, Canada

COMPRESSION BUCKLING OF THICK ORTHOTROPIC PLATES WITH A STEP THICKNESS CHANGE

Eric R. Johnson and Carlos G. Davila
Aerospace and Ocean Engineering
Virginia Polytechnic Institute and State University
Blacksburg, Virginia 24061-0203 USA

The buckling analysis of laminated plates with a step thickness change is important in the design of aircraft wing skins. Stiffness tailoring of wing skins made from filamentary composites can be accomplished by terminating internal plies along the span from root to tip. The terminated plies, or dropped plies, result in an abrupt thickness change. Buckling analyses using classical theory are presented by DiNardo and Lagace [1] for graphite/epoxy plates with dropped plies, and by Mikami, et al. [2] for orthotropic plates with a step thickness change. Both of these papers show that the buckling load of a plate with a step change in thickness is bounded from below by the buckling load of a uniform plate with the thickness of the thin section, and bounded from above by a uniform plate with the thickness of the thick section.

The purpose of this paper is to show the influence of transverse shearing deformations on the buckling of thick, specially orthotropic laminated plates with a step change in thickness. The example problem and nomenclature are shown in Fig. 1. A rectangular plate subjected to uniaxial compression with the step perpendicular to the load axis, spanning the width of the plate, and symmetric about the middle plane of the plate is shown in the figure. Buckling coefficents are presented for a simply supported square plate (a = b) with a centrally located step ($a_1 = a_2 = a/2$) as the thickness t_1 of one half is decreased relative to the thickness t_2 of the other half for a plate of constant weight. For a square plate of constant weight with a centrally located step, the sum of the thicknesses of the thin and thick sections is constant, and equal to twice the average thickness of the plate. The average thickness is denoted by t, and we consider two thickness-to-width ratios t/b = 0.1 and t/b = 0.2.

Laminate stiffnesses are computed for a three layer $[0/90/0]_T$ stacking sequence where the zero-degree fiber direction is along the load axis, and each layer is identical. The layer elastic properties are $E_L/E_T = 30$, $G_{LT}/E_T = 0.6$, $G_{TT}/E_T = 0.5$, $\nu_{LT} = \nu_{TT} = 0.25$, where L and T denote directions parallel and transverse to the fibers and ν_{LT} is the major Poisson's ratio. This cross-ply laminate is the same one considered in References [3] and [4], in which the effect of transverse shearing deformations on the compression buckling of uniform thickness plates were considered. The transverse shear stiffnesses A_{44} and A_{55} are computed under the assumptions of a uniform distribution of the transverse shear strains through the thickness, and a parabolic distribution of the corresponding shear stresses; see Eqn. (2.61) in Reference [5].

Values of the dimensionless buckling coefficient K as a function of t_1/t_2 for classical laminated plate theory (CLT), and for shear deformation theory (SDT) with t/b = 0.1 and t/b = 0.2 are shown in Fig. 2. The buckling coefficient is defined by

$$K = \bar{N}_{xcr} b^2 / (E_T t^3)$$

where $\bar{N}_{xcr}$ denotes the critical value of uniform compressive load intensity $\bar{N}_x$. The buckling coefficient for CLT is independent of the thickness ratio t/b [3].. It is clear from the figure that transverse shearing deformations have a significant effect on the buckling coefficient for these thick plates. However, the differences between K for CLT and SDT decrease as the ratio t_1/t_2 decreases from unity.

Plots of the out-of-plane displacement component of the buckling mode for $-0.5 \le x/a \le 0.5$ at y = b/2 are shown in Figs. 3 and 4. The buckling mode was normalized such that the maximum displacement is unity. In Fig. 3 the mode shapes are shown for SDT with t/b = 0.2 and for various ratios of t_1/t_2. For small values of t_1/t_2 a discontinuous slope in the displacement occurs at the step, and the majority of the strain energy due to buckling is stored in the thin section rather than the thick section. The buckling modes for CLT and SDT with t/b = 0.1 and 0.2 are shown for comparison in Fig. 4 with $t_1/t_2 = 0.75$. The slope is continuous at the step for CLT and for SDT with t/b = 0.1. For SDT with t/b = 0.2, however, the slope at the step is discontinuous. Thus, the buckling modes can be significantly different for SDT with respect to CLT.

Acknowledgment

This work was supported by NASA Grant NAG1-537.

References

1. DiNardo, M.T., and Lagace, P.A., "Buckling and Postbuckling of Laminated Composite Plates with Ply Dropoffs," in the Proceedings of the AIAA/ASME/ASCE/AHS 28th Structures, Structural Dynamics and Materials Conference, Monterey California, April 1987, pp. 156-164; AIAA Paper No. 87-0730.

2. Mikami, I., Dogaki, M., and Yonezawa, H., "Elastic Buckling of Orthotropic Plates with Abruptly Varying Rigidities under Compression," in Theoretical And Applied Mechanics, Vol. 24, Proceedings of the 24th Japan National Congress for Applied Mechanics, 1974, University of Tokyo Press, pp. 365-373.

3. Cohen, G.A., "Effect of Transverse Shear Deformation on Anisotropic Plate Buckling," Journal of Composite Materials, Vol. 16, July 1982, pp. 301-312.

4.Noor, A.K., "Stability of Multilayered Composite Plates," Fiber Science and Technology, Vol. 8, 1975, p.81.

5. Vinson, J.R., and Sierakowski, R.L., The Behavior of Structures Composed of Composite Materials, Martinus Nijhoff Publishers, 1986, p. 55.

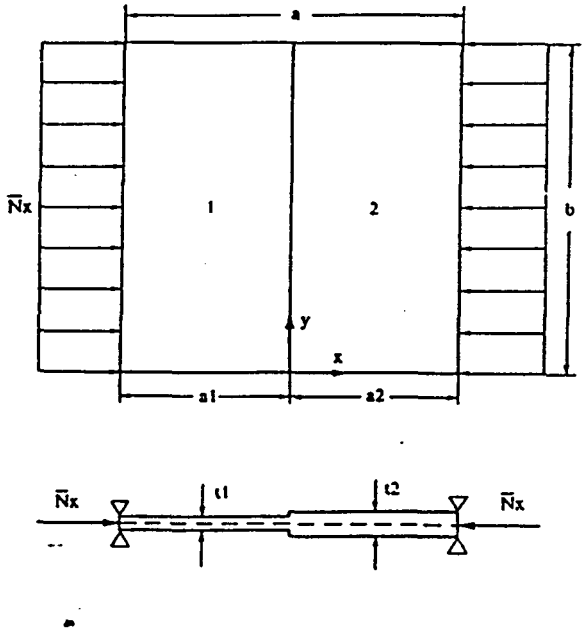

Fig. 1 In-plane compression of a rectangular plate with a symmetric step change in thickness

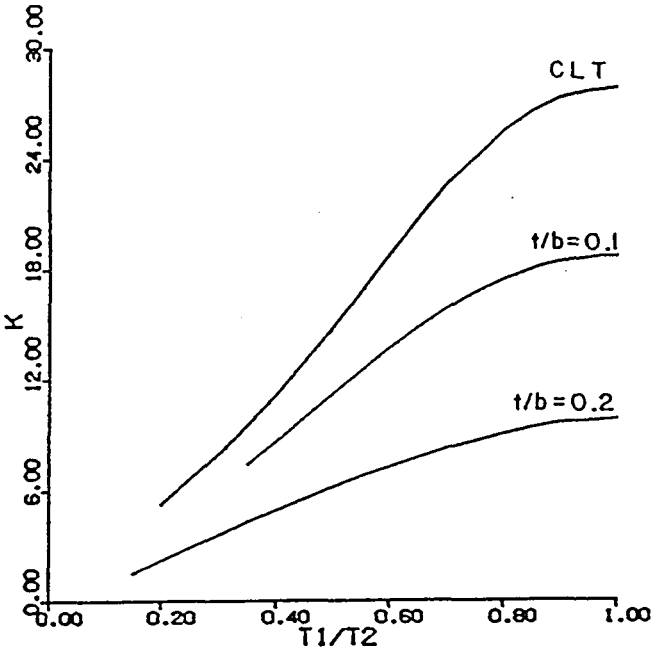

Fig. 2 Dimensionless buckling coefficient as a function of t_1/t_2 for CLT, SDT with t/b = 0.1, and SDT with t/b = 0.2

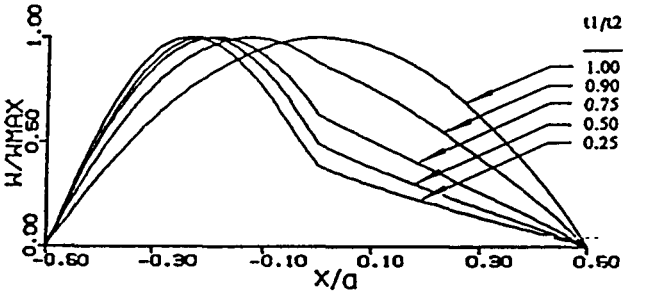

Fig. 3 Buckling modes for SDT with t/b = 0.2 and various ratios of t_1/t_2; y = b/2.

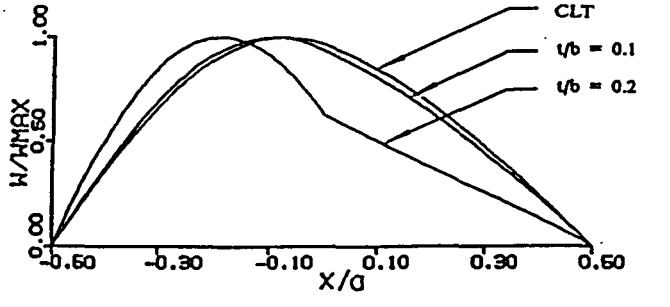

Fig.4 Buckling modes with t_1/t_2 = 0.75 for CLT, SDT with t/b = 0.1, and SDT with t/b = 0.2; y = b/2.